

Numerical study of magnetic field induced ordering in $\text{BaCuSi}_2\text{O}_6$ and related systems

Kwai-Kong Ng and Ting-Kuo Lee

Institute of Physics, Academia Sinica, NanKang, Taipei 11529, Taiwan

(Dated: November 20, 2018)

Thermodynamics of spin dimer system $\text{BaCuSi}_2\text{O}_6$ is studied using a quantum Monte Carlo calculation (QMC) and a bond-operator mean field theory. We propose that a new type of boson, which, rather than being hard-core, allows up to two occupancy at each site, is responsible for the Bose Einstein condensation of field induced ordering. Its superfluid density is identified as the square of the in-plane staggered magnetization m_{xy} in the ordered phase. We also compare our QMC result of the spin Heisenberg model to those predicted by mean field theory as well as by the simple hard core boson model for both large and small intra-dimer coupling J . The asymmetry of the phase diagram of $m_{xy}(h)$ of small coupling J in related systems such as $\text{NiCl}_2\text{-4SC}(\text{NH}_2)_2$ is explained with our new boson operator.

PACS numbers: 75.10.Jm, 75.40.Cx, 75.40.Gb, 75.40.Mg

I. INTRODUCTION

Recent experiment on $\text{BaCuSi}_2\text{O}_6$ under strong external magnetic field observed a λ -like transition of the specific heat capacity¹. This is among other spin dimer systems, such as KCuCl_3 and TlCuCl_3 , that exhibit quantum phase transition from spin liquid to a magnetically ordered state with increasing magnetic field. The ordered phase is characterized by an uniform magnetization accompanied by a long range staggered magnetic order perpendicular to the field. The staggered magnetization vanishes as temperature rises above the transition temperature T_c . This has been interpreted as a phenomenon of Bose-Einstein Condensation (BEC) of the magnetic field induced $S_z = +1$ triplets, which, when ignoring higher energy interactions, behave like repulsive hard-core bosons¹¹. The external field now plays the role of chemical potential and controls the number of triplets. Measurements of T_c near critical field h_c are reported to have the deduced critical exponent $\nu = 0.63(3)^2$, in good agreement with the predicted value $\nu = \frac{2}{3}$ of Bose-Einstein condensation. Numerical calculations also found the critical exponent approaching the expected as $h \rightarrow h_c$ ^{2,3} for 3D spin dimer systems, support the notion of BEC.

Previous numerical calculation on the hard-core boson model found a similar transition as observed¹. Instead, in this paper, we employ the original Heisenberg model to study the temperature and field dependence of thermodynamic quantities. In contrast to the hard-core model, we introduce a new type of boson, which allows up to two occupancy at each site, and show that its condensate density is identical to the staggered magnetization m_{xy}^2 in the ordered phase with the global phase corresponds to the direction of m_{xy} . The temperature and magnetic dependence of m_{xy}^2 is explained in the context of Bose-Einstein condensation. We also extend to the case with smaller inter-plane coupling in which higher energy states are no longer negligible in the ordered phase and leads to the asymmetry of on both $m_z(h)$ and $m_{xy}^2(h)$. This condition is relevant to other dimers material like TlCuCl_3

and $S = 1$ system $\text{NiCl}_2\text{-4SC}(\text{NH}_2)_2$ ^{4,5}.

II. MODEL HAMILTONIAN

In $\text{BaCuSi}_2\text{O}_6$, while Cu^{2+} ions arrange itself in layers of square lattice, every two Cu-Si-O layers are separated by planes of Ba^{2+} ions, and the distance between adjacent bilayers, 7.043 \AA^6 , is much larger than the bilayer separation, 2.73 \AA . Consequently, the spins of Cu^{2+} ions form dimers between bilayers and interact weakly in plane and out of plane. We study the antiferromagnetic Heisenberg model in an external field $h\hat{z}$ written as:

$$H_{sp} = J \sum_i \mathbf{S}_{1,i} \cdot \mathbf{S}_{2,i} + J_1 \sum_{\alpha, \langle i,j \rangle} \mathbf{S}_{\alpha,i} \cdot \mathbf{S}_{\alpha,j} + J_2 \sum_i \mathbf{S}_{1,i} \cdot \mathbf{S}_{2,i+\hat{z}} - \mu_B g_0 h \sum_{\alpha, i} S_{\alpha,i}^z, \quad (1)$$

where $\alpha = 1, 2$ denotes the layer index and the second summation refer to summing over all nearest neighbors in the xy plane for both types of layers. The exchange coupling constants are taken as $J = 4.45 \text{ meV}$, $J_1 = 0.58 \text{ meV}$ and $J_2 = 0.116 \text{ meV}$, which is provided by ref. 1 whose QMC based on the hard-core boson model using these parameters yield the best fit to the experimental result. The magnetic field h yields the Zeeman energy in the Hamiltonian and the gyromagnetic constant $g_0 = 2.306$ in the case of $\text{BaCuSi}_2\text{O}_6$. We first focus on the condition that $J \gg J_1, J_2$ so that the zero field ground state only composed of inter-plane singlet dimer states. Finite energy is needed to excite a singlet state $|s\rangle \equiv (|\uparrow\downarrow\rangle - |\downarrow\uparrow\rangle)/\sqrt{2}$ to a triplet state $|t_+\rangle \equiv |\uparrow\uparrow\rangle$. Increasing the magnetic field h will reduce the energy gap which closes up at a critical $h_c \sim 24 \text{ T}$ such that $\mu_B g_0 h_c$ is of order J . For $h > h_c$, a new magnetic order with staggered magnetization in the xy plane emerges, with the ground state a linear combination of $|s\rangle$ and $|t_+\rangle$ in each dimer. The breaking of rotational symmetry in the xy plane implies the existence of a Goldstone mode at $\mathbf{Q} = (\pi, \pi, \pi)$. Raising the field h

further leads to a finite transition temperature T_c which reaches a maximum before falls down again to zero at a saturation field h_s .

From another point of view, the quantum phase transition at h_c can be considered as BEC of bosons $b^\dagger \equiv t_{+1}^\dagger$ on the vacuum composed of $|s\rangle$. Since no more than one triplet is allowed in the same dimer, the triplet dimers b^\dagger , with $\mathbf{S}=+1$, behave as hard-core bosons. These bosons interact repulsively because J_1 and J_2 favor anti-ferromagnetic couplings of neighboring dimers and hence neighboring bosons are avoided. One can reduce H_{sp} to an effective Hamiltonian H_b ¹ of hard core bosons by projecting out higher energy states $|t_0\rangle \equiv (|\uparrow\downarrow\rangle + |\downarrow\uparrow\rangle)/\sqrt{2}$ and $|t_-\rangle \equiv |\downarrow\downarrow\rangle$,

$$\begin{aligned} H_b = & t_1 \sum_{\langle i,j \rangle} (b_i^\dagger b_j + h.c.) + V_1 \sum_{\langle i,j \rangle} n_i n_j \\ & + t_2 \sum_i (b_i^\dagger b_{i+\hat{z}} + h.c.) + V_2 \sum_i n_i n_{i+\hat{z}} \\ & + \mu \sum_i n_i, \end{aligned} \quad (2)$$

where $t_1 = V_1 = J_1/2$, $t_2 = V_2 = J_2/4$ and $n_i = b_i^\dagger b_i$. The chemical potential, $\mu = J - \mu_B g_0 h$, now depends on the magnetic field h and only when $h > h_c$, a finite concentration of bosons arises and condensate forms in the ground state. Note that this Hamiltonian preserves a particle-hole symmetry that the phase diagram of $T_c(h)$ (or $n_0(h)$, the superfluid density), must be symmetric about a h_m where T_c is a maximum at $n_0 = 1/2$. Numerical calculations based on this hard-core boson model reproduce thermodynamical quantities that agree well with the experimental results and support this boson picture¹. Matsumoto *et al.* pointed out that, however, when constructing a consistent mean field theory^{7,8}, the high energy state $|t_-\rangle$ should be included. This is reflecting the process of annihilating $|t_+\rangle$ and $|t_-\rangle$ at neighboring dimers while creating a $|s\rangle$ and vice versa. This process becomes important when the inter-dimer coupling J_1 and J_2 are comparable to intra-dimer coupling J and when h is not much larger than h_c . Therefore, to provide a consistent and general description for all J and h , we introduce the appropriate boson operator \tilde{b}^\dagger :

$$\tilde{b}_i^\dagger = \frac{(-1)^i}{\sqrt{2}} (S_{1,i}^+ - S_{2,i}^+), \quad (3)$$

with its operations on the spin states

$$\begin{aligned} \tilde{b}_i^\dagger |s\rangle_i &= |t_+\rangle_i & \tilde{b}_i |t_+\rangle_i &= |s\rangle_i \\ \tilde{b}_i^\dagger |t_+\rangle_i &= 0 & \tilde{b}_i |s\rangle_i &= |t_-\rangle_i \\ \tilde{b}_i^\dagger |t_-\rangle_i &= |s\rangle_i & \tilde{b}_i |t_-\rangle_i &= 0 \end{aligned}$$

for even i and an extra negative sign for odd i . Here $|t_+\rangle_i$ is redefined as $-|\uparrow\uparrow\rangle_i$, and the first and second arrows denote the spins of layer 1 and layer 2 respectively. These yield the expectation values $\langle s|\tilde{b}^\dagger \tilde{b}|s\rangle = \langle t_+|\tilde{b}^\dagger \tilde{b}|t_+\rangle = 1$

and $\langle t_-|\tilde{b}^\dagger \tilde{b}|t_-\rangle = 0$. Unlike b^\dagger , \tilde{b}^\dagger operates on a Hilbert space of vacuum $|0\rangle \equiv |t_-\rangle$, while $|s\rangle$ and $|t_+\rangle$ correspond to single and double occupied states of \tilde{b} respectively. $|t_0\rangle$ is again decoupled from the other states and not included in the Hilbert space. Although occupation greater than two at each lattice site is again prohibited, \tilde{b} boson is no longer the simple hard core boson described by b . Note that the vacuum is higher in energy and the lowest energy state $|s\rangle$ is fully occupied when $h < h_c$.

The modified effective Hamiltonian is now written as:

$$\begin{aligned} H_{\tilde{b}} = & \sum_i \epsilon (\tilde{b}_i^\dagger \tilde{b}_i + \tilde{b}_i \tilde{b}_i^\dagger) + \mu \sum_i \tilde{n}_i \\ & + t_1 \sum_{\langle i,j \rangle} (\tilde{b}_i^\dagger \tilde{b}_j + h.c.) + V_1 \sum_{\langle i,j \rangle} \tilde{n}_i \tilde{n}_j \\ & + t_2 \sum_i (\tilde{b}_i^\dagger \tilde{b}_{i+\hat{z}} + h.c.) + V_2 \sum_i \tilde{n}_i \tilde{n}_{i+\hat{z}}, \end{aligned} \quad (4)$$

where $\epsilon = -J$, $\mu = -\mu_B g_0 h$ and $\tilde{n}_i = \tilde{b}_i^\dagger \tilde{b}_i - \tilde{b}_i \tilde{b}_i^\dagger$ with $t_{1,2}$ and $V_{1,2}$ unchanged. The potential energy terms arise from the term $S_i^z S_j^z$ of the original spin Hamiltonian H_{sp} which is attractive for t_+ and t_- but is repulsive for the same kind of triplets. This Hamiltonian now loses the symmetry between $|s\rangle$ and $|t_+\rangle$ due to the presence of $|t_-\rangle$. For $h_c < h < h_s$, it is the condensation of this boson \tilde{b} that gives the quantum phase transition observed.

III. MEAN FIELD THEORY

A mean field condensate ground state of the effective Hamiltonian $H_{\tilde{b}}$ is written as⁷

$$\begin{aligned} |\Psi_0\rangle = & \prod_i \left(u \tilde{b}_i^\dagger + v (-1)^i (f e^{i\theta} \tilde{b}_i^{\dagger 2} + g e^{-i\theta}) \right) |0\rangle_i, \\ = & \prod_i (u |s\rangle_i + v (-1)^i (f e^{i\theta} |t_+\rangle_i + g e^{-i\theta} |t_-\rangle_i)) \end{aligned} \quad (5)$$

where $u^2 + v^2 = 1$ and $f^2 + g^2 = 1$ and all parameters are real. The last equation is exactly the same as the one taken for mean field condensate using bond operator representation⁷ in which θ is chosen to be zero. The global phase θ corresponds to the angle of rotation in the xy -plane whose presence, due to the rotational invariance, should not change the energy of the system. t_+ and t_- undergo the transformation $t_+ \rightarrow e^{i\theta} t_+$ and $t_- \rightarrow e^{-i\theta} t_-$ when the x and y axes are rotated by an angle θ . As shown below, this phase θ also specifies the orientation of the in-plane staggered magnetization.

Remarkably, the ground state $|\Psi_0\rangle$ has two finite expectation values that correspond to two order parameters:

$$\langle \tilde{b} \rangle = u v (f + g) e^{i\theta} \equiv \tilde{b}_0 e^{i\theta} \quad (6)$$

$$\langle \tilde{b}^2 \rangle = v^2 f g e^{2i\theta}. \quad (7)$$

The first one is the usual order parameter expected from a BEC, while the second additional one is originated from

the fact that \tilde{b} allows up to two bosons occupied at each site i . These expectation values can be related to the staggered magnetization and spin-spin correlation function when Eq. 3 is applied.

In the spin language, the staggered magnetization is taken as the order parameter for the ordered phase and defined as

$$m_{xy}^2 = m_x^2 + m_y^2, \\ m_\alpha = \frac{1}{N\sqrt{2}} \sum_i (-1)^i \langle S_{1,i}^\alpha - S_{2,i}^\alpha \rangle \quad \alpha = x, y.$$

As mentioned above, one can easily show that m_{xy} is identical to the magnitude of superfluid order parameter \tilde{b}_0 . Using the definition of \tilde{b}^\dagger from Eq. 3, one obtains

$$m_x = \frac{1}{2N} \sum_i \langle \tilde{b}_i^\dagger + \tilde{b}_i \rangle \\ = \tilde{b}_0 \cos \theta.$$

Similarly, $m_y = \tilde{b}_0 \sin \theta$ and consequently,

$$m_{xy} = \tilde{b}_0 = uv(f + g), \quad (8)$$

and the phase θ specifies the direction of m_{xy} . The realization of $m_{xy} = \tilde{b}_0$ allows us to compute the staggered magnetization directly using QMC.

The uniform magnetization along \hat{z} axis m_z can also be written as

$$m_z = \frac{1}{N} \sum_i \langle \tilde{b}_i^\dagger \tilde{b}_i - \tilde{b}_i \tilde{b}_i^\dagger \rangle \\ = v^2(f^2 - g^2), \quad (9)$$

which is simply the difference between the number of $|t_+\rangle$ and of $|t_-\rangle$.

We stress that the distinction between \tilde{b}^\dagger and b^\dagger originates from the consideration of $|t_-\rangle$, which we take as the vacuum here. If the $|t_-\rangle$ state is much higher in energy and being ignored, \tilde{b}^\dagger , as $g \rightarrow 0$, is just the hard core boson b^\dagger described in ref. 1. This approximation becomes exact when $J \rightarrow \infty$, but will be insufficient when $J \sim J_1, J_2$.

A complete description of the static and dynamical properties of BaCuSi₂O₆ under applied field can be obtained by performing a mean field analysis using the bond operator representations. The same method has been successfully applied to related compounds of KCuCl₃ and TiCuCl₃ by Matsumoto *et al.*⁷

Under bond operator representations, each spin operator is replaced by boson operators, one singlet and three triplet operators, that operate on a inter-plane dimer bond and the original spin Hamiltonian is then transformed to a Hamiltonian of interacting bosons. These are hard core bosons because of the constraint $1 = s^\dagger s + t_+^\dagger t_+ + t_0^\dagger t_0 + t_-^\dagger t_-$. Two unitary transformations are performed to mix the bond operators in the ordered phase to give the appropriate condensate $\bar{a} = \langle a_i \rangle_{av}$,

$$a_i = us_i + ve^{-i\mathbf{Q} \cdot \mathbf{r}_i} (f e^{i\theta} t_{+i} + g e^{-i\theta} t_{-i}).$$

For convenience we set $\theta = 0$. This ground state condensate is in fact identical to $|\Psi_0\rangle$. The mean field approach proceeds as usual by taking the a_i as a uniform field \bar{a} and minimizing the energy to obtain a set of self-consistent equations. The parameters u, v, f and g are now determined by the self-consistent equations. The particle number constraint does pose a problem on the decoupling of operators in the above procedure. Naively employing a Lagrange multiplier to account for the constraint would not close the energy gap in the ordered phase. In ref. 7 a Holstein-Primakoff approximation is taken instead by assuming the contribution of energy modes other than a_i is small in the ground state. This approach successfully recovered the Goldstone mode with expected features for the ground state. We refer the readers to ref. 7 for the details and only present our result here.

IV. QUANTUM MONTE CARLO CALCULATION

The aim of quantum Monte Carlo simulations is twofold: to test the validity of the proposed mean field theory and to justify the hard-core boson model. We stress that the simulations are performed on the original spin Heisenberg model rather than the boson model and any observed phase transition is a pure consequence of spin exchange coupling of H_{sp} .

Having been successfully applied to spin systems in external magnetic field in the last decade and demonstrated its advantages over the standard worldline approach, the stochastic series expansion (SSE)⁹ is the method of choice for our problem. The algorithm of measuring Green's function introduced by Dorneich *et al.*¹⁰ allows us to compute the spin correlations like $\langle S_i^+ S_j^- \rangle$. In this scheme, however, since spin must be conserved in the ensemble, direct measurement of staggered magnetization m_{xy} , which requires the knowledge of $\langle S_i^+ \rangle$ and $\langle S_i^- \rangle$, is impossible. Instead, in our calculation, we compute the superfluid density

$$n_0 = \frac{1}{N^2} \sum_{i,j} \langle \tilde{b}_i^\dagger \tilde{b}_j \rangle. \quad (10)$$

In MFT, Eq. 6 and Eq. 8 lead to $n_0 = \tilde{b}^2 = m_{xy}^2$, and to which our simulated n_0 can be compared. Using the definition of \tilde{b} , Eq. 3, the computation of n_0 involves only measuring spin correlations which can be done easily with Dorneich's method. Therefore a direct comparison of the calculated order parameter by QMC to those predicted by mean field approximation as well as experimental data is possible.

All simulations are performed on cubic lattice of size 12x12x12 typically with 4×10^5 update measurement cycles for each data point, except the measurement of specific heat which requires up 1.6×10^6 update cycles to achieve the acceptable accuracy.

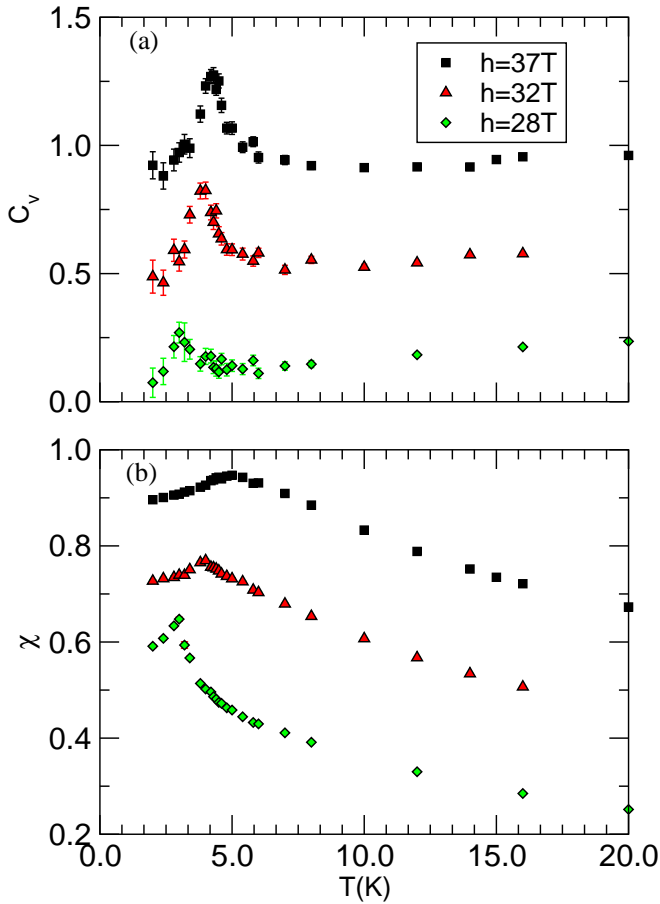


FIG. 1: (color online) QMC result of (a) specific heat c_v and (b) spin susceptibility χ vs. temperature for different magnetic fields. Data for different h are shifted for clarity.

V. THERMODYNAMICS

The specific heat and susceptibility at finite temperature around the transition have been experimentally measured by Jaime *et al.*¹ for various magnetic fields. The sharp peak of specific heat at T_c has a familiar λ shape similar to the one found in liquid helium He⁴. Our QMC calculations based on the spin Hamiltonian H_{sp} reproduce this result for different h as shown in Fig. 1(a). A peak of the specific heat c_v signals the BEC develops when $h > h_c$ ($h_c \sim 24\text{ T}$) and the peak grows with increasing T_c as h is increased. The calculated values of T_c approximately agree with the experimental result. For $h = 37\text{ T}$, our calculated and the experimental T_c are $\sim 4\text{ K}$ and $\sim 3.75\text{ K}$ respectively¹. Remind that we adopted the parameters J , J_1 and J_2 used in ref. 1 in which the hard-core boson Hamiltonian H_b was used to reproduce the experimental result. Therefore the discrepancy on T_c between QMC and experiment is a consequence of ignoring higher energy states in H_b . One can certainly produce a better fit to the experimental data if different couplings than those obtained by ref. 1 are used.

The calculated spin susceptibility χ_s in Fig. 1(b) also

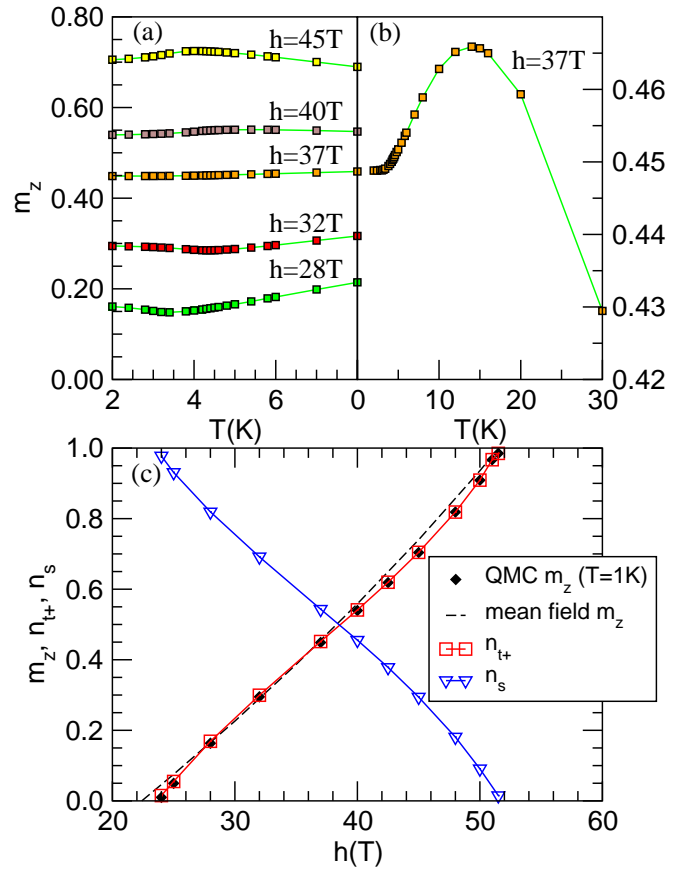


FIG. 2: (color online) (a) Low temperature regime of uniform magnetization per dimer m_z for different magnetic fields that exhibits BEC. (b) The whole temperature range of m_z for field $h = 37\text{ T}$. (c) Magnetic field dependence of m_z obtained from both QMC ($T = 1\text{ K}$) and MFT together with the number density of s and t_+ states.

shows a peak at T_c . The formation of boson condensate below T_c freezes the spins in the condensate and therefore reduces the response to the external field that leads to a drop in χ_s . Unlike the specific heat, the transition peak reduces when h increases and becomes rather flat at $h \sim h_m$.

The phase transition is also visible in the low temperature regime of uniform magnetization in which a minimum (maximum) is reached at T_c for $h < h_m$ ($h > h_m$) as displayed in Fig. 2(a). For $h < h_m$, the low-lying energy states have the $|s\rangle$ state dominating and so as T approach T_c from above, m_z , which is approximately equal to the number of t_+ states, reduces. However, below T_c , due to the formation of superfluid condensate, number of t_+ states increases as the fraction of condensate grows and therefore raises the m_z . This feature is also found in the attractive Hubbard model of electrons¹⁵ in which the double occupancy, i.e. the number of on-site Cooper pairs, increases as T approaches 0 from T_c .

The role of s and t_+ states exchanges for $h > h_m$ and a maximum of m_z is resulted instead. The same tem-

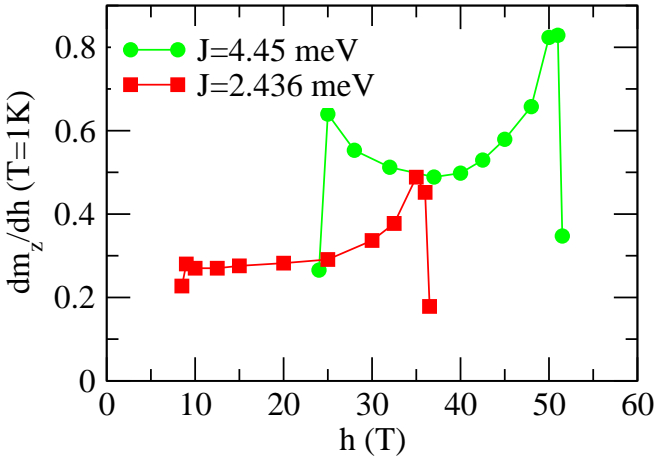


FIG. 3: (color online) The slope of $m_z(h)$, i.e. the susceptibility, at $T = 1\text{K}$.

perature dependence of magnetization was also observed in another dimer system TiCuCl_3 ¹² experimentally and a Hartree-Fork calculation¹³ on hard core dilute magnons explained the qualitative feature of $m_z(T)$ around T_c of the proposed BEC. QMC simulations on different coupling strength¹⁴ has shown that this is a general feature of 3D coupled dimer system while the extrema are missing in non-interacting dimers.

Since the total uniform magnetization is simply the difference between the number of $|t_+\rangle$ state and of $|t_-\rangle$, further increase of temperature (to $T \sim 15\text{ K}$ for $h = 37\text{ T}$) will raise the number of $|t_-\rangle$, as well as $|t_0\rangle$ and finally suppresses the magnetization m_z as shown in Fig. 2(b).

In Fig. 2(c) we plot the field dependence of m_z obtained by both QMC and MFT, which increases monotonically as h increases, consistent to experimental results. While $m_z(h)$ is more or less linear in the mean field case, its slope reduces and then increases in the QMC calculation. This change of slope is again a consequence of the formation of condensate. Without the condensation, $m_z(h)$ will be simply a straight line at $T = 0$. But the formation of condensate below T_c increases m_z for $h < h_m$ as discussed above. While the minimum of $m_z(T)$ disappears at h_c ($T_c = 0$) and h_m , there is no increase of magnetization due the condensation at these two fields. Therefore the resulted $m_z(h)$ curve for $h < h_m$ must be convex as shown. Similar argument applies to the high field regime $h > h_m$ and a concave curve is predicted. The slope of $m_z(h)$, that is the susceptibility, is shown in Fig. 3. The small asymmetry indicates the existence of t_- states which becomes more significant for smaller intra-dimer coupling J as will be discussed in the next section.

Also plot in Fig. 2(c) is n_{t+} and n_s , the average number of triplet t_+ and singlet s per dimer respectively. In the MFT, $n_{t+} = v^2 f^2$, $n_{t-} = v^2 g^2$ and $n_s = u^2$, where u , v , f and g are parameters given by the condensate ground state $|\Psi_0\rangle$ (Eq. 5). n_{t-} is found to be negligi-

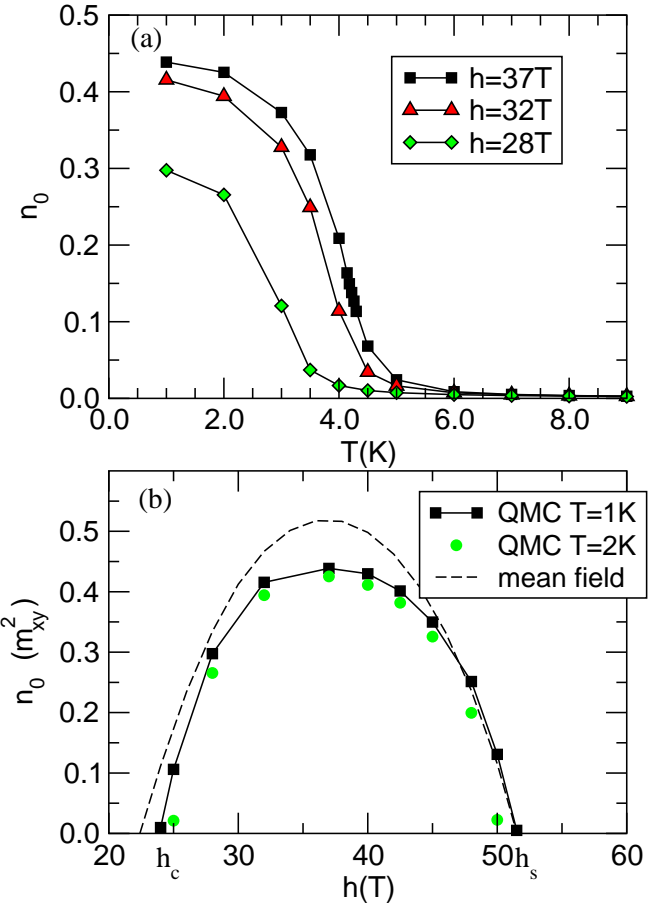


FIG. 4: (color online) Superfluid density n_0 , which is equivalent to m_{xy}^2 in the MFT, as (a) a function of temperature and (b) a function of magnetic fields.

ble and therefore is not shown in Fig. 2(c). While n_s reduces as n_{t+} increases, their total number is almost 1 (less than 2 percent in difference) for all fields. The intercept of both curves gives an estimate of $h_m = 38.6\text{ T}$ in which $n_{t+} \approx n_s \approx 0.5$.

The fact that n_{t+} essentially coincides with m_z means the average number of t_- is almost zero (g^2 is very small) in $\text{BaCuSi}_2\text{O}_6$. This explains why the hard-core boson model b gives results consistent to experimental data. However, the derivation from the hard-core boson model will be more apparent when we discuss the m_{xy} where the difference is proportional to g instead of g^2 .

Temperature dependence of n_0 is shown in Fig. 4. n_0 , equivalent to the superfluid density m_{xy}^2 in MF, starts to rise at about the same T_c obtained from specific heat and spin susceptibility and therefore justifies the idea of BEC of \tilde{b}^\dagger for the transition observed in $\text{BaCuSi}_2\text{O}_6$. The broken rotational symmetry below T_c that generates m_{xy} is identical to the broken gauge invariance of $|\Psi_0\rangle$. Also shown in Fig. 4 is the field dependence of m_{xy}^2 at low temperature. The data shows that although MF calculation overestimates the order parameter near the field h_m , in general it agrees well with QMC result. The predicted

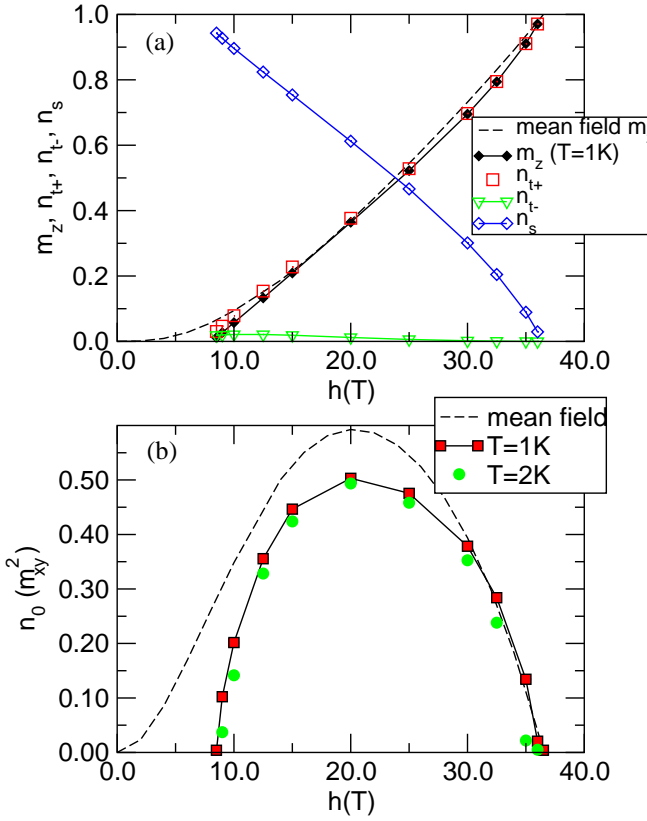


FIG. 5: (color online) Results of reduced inter-plane coupling $J = 2.436$ meV. (a) Temperature dependence of m_z and number density of s , t_+ and t_- states. (b) Phase diagram of $n_0(h)$.

MF values of critical and saturation fields are given by:

$$\begin{aligned}\mu_B g_0 h_c &= \sqrt{J(J - 4J_1 - 2J_2)} \\ \mu_B g_0 h_s &= J + 4J_1 + 2J_2.\end{aligned}$$

Since quantum fluctuation is totally surpassed in the fully polarized phase, mean field theory predicts the exact saturated field h_s as expected. Below h_s , quantum fluctuation stabilizes the disordered state and so reduces the order parameter away from the MF value. The small discrepancy around h_c will become more significant when we lower the inter-plane coupling J where MF gives a much smaller h_c than the true value. It is also obvious that m_{xy}^2 is asymmetric about h_m , contrast to what is predicted by the hard-core boson model that retains a particle-hole symmetry. This indicates that t_- states, although the average number is small, does play a measurable role in the ordered phase.

VI. REDUCED EXCHANGE COUPLING J

In $\text{BaCuSi}_2\text{O}_6$, since J_1/J and J_2/J are relatively small, the mixing of $|t_-\rangle$ state is not significant, as least for $h \gg h_c$. But there are other dimer systems, like TiCuCl_3 , where inter-dimer coupling is strong enough

that significant mixing of $|t_-\rangle$ is expected and new features are possible. Therefore we extend our study to smaller intra-dimer coupling J on the same bilayer lattice as in $\text{BaCuSi}_2\text{O}_6$. One possibility to reduce J experimentally is the substitution of Si by atoms of larger radius but the same chemical valence, in order to enlarge the intra-dimer distance. Germanium, the one right below Si in the period table, is the most natural candidate.

Reducing J also implies the reduction of h_c because triplet states have lower energies with small J . We choose the reduced J to be $J = 2.436$ meV such that the critical field h_c predicted by MFT is exactly zero. The calculated curve (Fig. 5) of $m_z(h)$ of MFT and QMC lay close to other each although QMC yields a finite h_c instead of zero. The average number of t_- is not negligible any more in this case. n_0 , or m_{xy} , shows a much larger discrepancy between QMC and MFT than the large coupling J case. MFT overestimates m_{xy} for a large range of magnetic field and only when close to the saturation field h_s that MFT is close to exact results. The asymmetry of m_{xy} is also enhanced when J is reduced as expected. Although n_- is still very small that m_z deviates only slightly from n_+ , the square root of it, $\sqrt{n_-} = vg$, can be as large as 0.14 and hence implies that H_b is not valid any more. The change of slope of $m_z(T)$ is also observable but is significantly asymmetric around $h_m \sim 20$ T as shown in Fig. 3.

Here we discuss how our results of reduced J can be successfully applied to a related compound $\text{NiCl}_2 \cdot 4\text{SC}(\text{NH}_2)_2$ (DTN)^{4,5}. Although this material is not a spin dimer system, the single ion anisotropy ($D \sim 0.88$ meV) plays the role J and splits the Ni $S = 1$ spin state into $S_z = 0$ and $S_z = \pm 1$ states, which corresponds to s and t_{\pm} states in the above discussion. Under an external magnetic field the same field induced ordering has recently been observed experimentally in DTN^{4,5}. In this case, our proposed condensate wave function becomes exact due to the absence of a corresponding t_0 state. Therefore the field induced transition observed in DTN shares the same physics as in spin dimer systems just described. Since $D \sim 0.88$ meV is comparable to the average exchange coupling $J' \sim 0.66$ meV, a large asymmetry in the phase diagram is expected as we considered in the dimer system. Recent experimental data indeed showed strong asymmetry in $T_c(h)$ as well as in the change of slope of magnetization curve. Instead of the proposed lattice expansion in the compound⁵, the anomalous change of slope in magnetization is in fact a consequence of the formation of superfluid condensate which either enhances or reduces m_z according to the applied field.

VII. SUMMARY

Working on the original antiferromagnetic Heisenberg model, our QMC calculations reproduce the experimental finding of the field induced ordering observed in both specific heat and spin susceptibility. The calculated c_v

shows a λ -like transition at T_c with the amplitude maximizes at $h \sim h_m$ and reduces to zero as h approaches h_c or h_s . This phenomenon can also be described as a Bose-Einstein condensation of magnons. Instead of hard-core boson, we propose a semi-hard-core boson, for which up to two occupancy is allowed, is responsible for the field induced condensation. We showed that the superfluid density n_0 is identical to the in-plane staggered magnetization m_{xy}^2 , which is the order parameter in the spin language. Our QMC results show a rise of $n_0 = m_{xy}^2$ at the same T_c of c_v and justify the idea of Bose-Einstein condensation. Due to the smallness of J_1 and J_2 in $\text{BaSiCu}_2\text{O}_6$, the number of t_- states is tiny and leads to the success of hard-core boson model H_b . Nevertheless, the inadequacy of H_b is still observable from the asymmetry of the phase diagram. A bond operator mean field approach agrees well with QMC data of m_z for all field, and of m_{xy}^2 for magnetic field close to h_c and h_s . Quantum fluctuations that ignored in the MFT lead to an overestimated m_{xy}^2 around h_m however. The difference is more significant as one considers a smaller inter-plane coupling J . MFT predicts a much smaller h_c than the value found by the QMC. The asymmetry of m_{xy}^2 is also much enhanced and signals the failure of simple hard-core boson model. This is indeed the case observed in $\text{NiCl}_2\text{-4SC}(\text{NH}_2)_2$. The condensation of magnons also leads to the change of slope in $m_z(h)$ which is again symmetric

around h_m when J is large but becomes asymmetric for smaller J systems such as observed in $\text{NiCl}_2\text{-4SC}(\text{NH}_2)_2$.

In the ordered phase, the bond operator mean field theory successfully account for longitudinal fluctuation, which is absent in the conventional mean field theory, in addition to the transverse fluctuation. The longitudinal fluctuation, or the spin amplitude mode, mixes with the transverse fluctuation, the phase mode, at lower field but becomes dispersionless and separated from the phase mode at higher field. However, topological excitation, corresponds to vortices of the condensate, can not be described in the framework of bond operator MFT and further work will be needed. Recently a BEC of magnons in frustrated triangular lattice of antiferromagnet has been proposed and a similar λ -transition in specific heat is also observed¹⁶. It raises the question whether the BEC is a more general phenomenon of quantum antiferromagnet in external field and also raises the possibility of some novel phenomena arising from quantum nature of the condensate.

Acknowledgments

We acknowledges financial support by the NSC (R.O.C.), grant no. NSC 93-2112-M-001-018.

¹ M. Jaime, V.F. Correa, N. Harrison, C.D. Batista, N. Kawashima, Y. Kazuma, G.A. Jorge, R. Stein, I. Heinmaa, S.A. Zvyagin, Y. Sasago, and K. Uchinokura, Phys. Rev. Lett. **93**, 87203 (2004).

² S.E. Sebastian, P.A. Sharma, M. Jaime, N. Harrison, V. Correa, L. Balicas, N. Kawashima, C.D. Batista, and I.R. Fisher, cond-mat/0502374.

³ O. Nohadani, S. Wessel, B. Normand, and S. Haas, Phys. Rev. B **69**, 220402(R) (2004).

⁴ A. Paduan-Filho, X. Gratens, and N.F. Oliveira, Jr., Phys. Rev. B **69**, 020405(R) (2004).

⁵ V.S. Zapf, D. Zocco, M. Jaime, N. Harrison, A. Lacerda, C. D. Batista, and A. Paduan-Filho, cond-mat/0505562.

⁶ L. W. Finger, R. M. Hazen, and R. J. Hemley, Am. Mineral. **74**, 952 (1989).

⁷ M. Matsumoto, B. Normand, T. M. Rice, and M. Sigrist, Phys. Rev. Lett., **89**, 077203 (2002), Phys. Rev. B **69**, 054423 (2004).

⁸ T. Sommer, M. Vojta, and K.W. Becker, Eur. Phys. J. B **23** 329 (2001).

⁹ A.W. Sandvik, Phys. Rev. B **59**, R14157 (1999), Phys. Rev. B **56**, 11678 (1997). O.F. Syljuåsen and A.W. Sandvik, Phys. Rev. E **66**, 046701 (2002).

¹⁰ A. Dorneich and M. Troyer, Phys. Rev. E **64**, 066701 (2001).

¹¹ T. Giamarchi and A. M. Tsvelik, Phys. Rev. B **59**, 11398 (1999).

¹² A. Oosawa, M. Ishii, and H. Tanaka, J. Phys. Condens. Matter **11**, 265 (1999).

¹³ T. Nikuni, M. Oshikawa, A. Oosawa, and H. Tanaka, Phys. Rev. Lett. **84**, 5868 (2000).

¹⁴ S. Wessel, Maxim Olshanii, and S. Haas, Phys. Rev. Lett. **87**, 206407 (2001).

¹⁵ J.M. Singer, M.H. Pedersen, T. Schneider, H. Beck, and H.G. Matuttis, Phys. Rev. B **54**, 1286 (1996).

¹⁶ R. Radu, H. Wilhelm, V. Yushankhai, D. Kovrizhin, R. Coldea, Z.Tylczynski, T. Luehmann, and F. Steglich, cond-mat/0505058.